# EPR Spectra of *trans*-$V(CO)_4(PMe_3)_2$ in a Single Crystal of *trans*-$Cr(CO)_4(PMe_3)_2$†

J. M. McCall, J. R. Morton,* and K. F. Preston

*Division of Chemistry, National Research Council of Canada, Ottawa, Ontario, Canada K1A 0R9*

*Received July 5, 1984*

EPR spectra of *trans*-$V(CO)_4(PMe_3)_2$ have been observed in a single crystal of *trans*-$Cr(CO)_4(PMe_3)_2$. The constants of the spin Hamiltonian suggest that the $d^5$ species has a $^2B_{2g}$ ground state in $D_{2h}$ symmetry. By comparison with data for $V(CO)_6$, it is concluded that the latter also possesses a $^2B_{2g}$ ground state, albeit contaminated by the nearby $^2B_{1g}$ state.

## Introduction

In 1981 we discussed the EPR spectrum and structure of $V(CO)_6$ doped into a single crystal of $Cr(CO)_6$.[1] Our interpretation of these data was not without certain ambiguities which we have, in the intervening period, been anxious to resolve. In particular, $V(CO)_6$ is a Jahn–Teller molecule,[2] and we concluded[1] that the distortion from octahedral geometry was an elongation of the V–C bonds directed along ±$z$. Others[3] reached the opposite conclusion, i.e., that the distortion was a $z$ axis compression followed by a further distortion to $D_{2h}$ symmetry.

We selected *trans*-$V(CO)_4(PMe_3)_2$ as an analogue of $V(CO)_6$ having a well-defined $z$ axis (the PVP direction), in the hope that the analysis of its EPR spectrum would shed some light on the interpretation of the spectrum of $V(CO)_6$.

## Experimental Section

A mixture of *cis*- and *trans*-$Cr(CO)_4(PMe_3)_2$ was prepared according to a published route.[4] Sublimation at 30–35 °C in vacuo gave large yellow (trans) and small colorless (cis) crystals which were easily separated by hand. Their conformation was confirmed by IR spectroscopy[4] and by X-ray crystallography.[5] A manuscript on their crystal structures is in preparation;[5] *trans*-$Cr(CO)_4(PMe_3)_2$ is monoclinic ($P2_1/c$) having $a = 6.856 \pm 0.002$ Å, $b = 8.610 \pm 0.007$ Å, $c = 13.715 \pm 0.004$ Å, $\beta = 103.5° \pm 0.01$, and $Z = 2$.

In contrast to the air-stable chromium derivative, $V(CO)_4(PMe_3)_2$ is extremely air-sensitive, and its preparation was carried out under an atmosphere of argon. A Schlenk storage tube was charged with 0.023 g (0.11 mmol) of $V(CO)_6$, 0.019 g (0.25 mmol) of $PMe_3$, and 10 mL of isopentane previously dried over type 4Å molecular sieve. The reactants were stirred in vacuo under subdued light for 21 h. Filtration gave a yellow filtrate from which we unsuccessfully attempted to isolate *trans*-$V(CO)_4(PMe_3)_2$. Finally, a portion of the filtrate was transferred to a sublimer containing excess *trans*-$Cr(CO)_4(PMe_3)_2$. After removal of the solvent at 0 °C, sublimation at 30–35 °C gave large, air-stable, orange crystals of *trans*-$Cr(CO)_4(PMe_3)_2$ containing ca. 0.2% of the vanadium analogue. The vanadium-doped crystals of *trans*-$Cr(CO)_4(PMe_3)_2$ were mounted on a two-circle goniometer[6] for examination at −180 °C in the EPR spectrometer.

A Varian E12 EPR spectrometer equipped with a variable-temperature accessory and frequency and magnetic field measuring devices was used to examine the vanadium-doped *trans*-$Cr(CO)_4(PMe_3)_2$ single crystals.

## Results

When doped into *trans*-$Cr(CO)_4(PMe_3)_2$ crystals, *trans*-$V(CO)_4(PMe_3)_2$ exhibited a spectrum (Figure 1) whose hyperfine interactions were always those of a single $^{51}V$ and *two equivalent* $^{31}P$ nuclei. A doped crystal was mounted on a two-circle goniometer and manipulated so that the magnetic field explored in turn the $a^*c$, $a^*b$, and $bc$ planes of the monoclinic crystal. This enabled us to plot $g^2$ and the hyperfine interactions $ga^2g/\mathrm{MHz}^2$ (Figure 2) as a function of angle and so assemble the correponding tensors.[6] In the $a^*c$ plane the spectra of the two sites which are always present in a monoclinic crystal were superimposed, whereas in the $a^*b$ and $bc$ planes the two sites were distinct and generated opposite signs in the corresponding tensor elements. The hyperfine tensors $a^2/\mathrm{MHz}^2$ were obtained by pre- and post-multiplying the tensors of $ga^2g$ by $g^{-1}$, the reciprocal of the $g$ tensor. The tensors of $g^2$, $ga_V{}^2g$, and $ga_P{}^2g$, together with the principal values and direction cosines of $g$, $a_V$, and $a_P$, are given in Table I.

The signs of the $a^*c$ off-diagonal elements of the tensors in Table I were determined directly from the exploration of the $a^*c$ plane (Figure 2). However, there remained ambiguity in the relative signs of the $a^*b$ and $bc$ elements of the tensors. This ambiguity was resolved by using the two-circle goniometer to place $H_0$ along $(3^{-1/2}, 3^{-1/2}, 3^{-1/2})$ and comparing the observed spectrum with the various predictions.[6] For the sign choice shown in Table I, excellent agreement with experiment was obtained. The other sign combinations gave poor agreement.

## Discussion

In Figure 3 we show the effect on the 3d energy levels of an octahedral molecule of trans substitution along the $z$ axis. For weakly $\sigma$-bonding ligands the effective result is that of $z$ axis elongation (Figure 3a). The resulting ground state for a low-spin $d^5$ species is $^2B_{2g}$ in $D_{4h}$ symmetry, and the $g$ tensor should be axially symmetric with a large, positive $\Delta g_\perp$. There is no compelling reason to postulate lower symmetry, and the present results for *trans*-$V(CO)_4(PMe_3)_2$ do not therefore conform to this model. Trans substitution by a strong $\sigma$-donor such as $PMe_3$ might be expected to correspond to $z$ axis compression, as indicated in Figure 3c. The fifth electron then enters the $e_g$ orbital, and with a Jahn–Teller distortion to $D_{2h}$ the situation in Figure 3d results.

As indicated, the $b_{3g}$ and $b_{2g}$ components of the putative $e_g$ level are connected by the spin-orbit interaction, since $R_z$ (rotation about $z$) belongs to the representation of the product of $B_{3g}$ and $B_{2g}$ in $D_{2h}$. This accounts for the large positive $g$ shift when $H_0$ lies along the $z$ axis. A smaller positive $g$ shift occurs when $H_0$ is placed along $y$ because

---

† NRCC No. 24348.

(1) Boyer, M. P.; LePage, Y.; Morton, J. R.; Preston, K. F.; Vuolle, M. J. *Can. J. Spectrosc.* **1981**, *26*, 181.

(2) Ammeter, J. H.; Zoller, L.; Bachmann, J.; Balzer, P.; Gamp, E.; Bücher, R.; Deiss, E. *Helv. Chim. Acta* **1981**, *64*, 1063.

(3) Bratt, S. W.; Kassyk, A.; Perutz, R. N.; Symons, M. C. R. *J. Am. Chem. Soc.* **1982**, *104*, 490.

(4) Jenkins, J. M.; Verkade, J. G. *Inorg. Chem.* **1967**, *6*, 2250.

(5) McCall, J. M.; LePage, Y., to be submitted for publication.

(6) Morton, J. R.; Preston, K. F. *J. Magn. Reson.* **1983**, *52*, 457.

0276-7333/85/2304-1272$01.50/0

**Table I. The Tensors of $g^2$, $ga_V{}^2g$/MHz$^2$, and $ga_P{}^2g$/MHz$^2$ of *trans*-$V(CO)_4(PMe_3)_2$ in a Single Crystal of *trans*-$Cr(CO)_4(PMe_3)_2$ Together with the Principal Values of $g$, $a_V$, and $a_P$ and Their Direction Cosines in the $a^*bc$ Axis System**

| | tensor | | | principal values and direction cosines of $g$ and $a$ | | |
|---|---|---|---|---|---|---|
| | | | | $x$ | $y$ | $z$ |
| | | | | 2.0002 | 2.0244 | 2.0419 |
| | 4.1171 | ∓0.0244 | 0.0239 | −0.1047 | 0.8416 | 0.5298 |
| $g^2$ | ∓0.0244 | 4.1235 | ∓0.0559 | ±0.3949 | ±0.5241 | ∓0.7546 |
| | 0.0239 | ∓0.0559 | 4.0277 | 0.9127 | −0.1302 | 0.3873 |
| | | | | 91.7[a] | 218.2[a] | 83.9[a] |
| | 137580 | ±59763 | −49241 | 0.4816 | 0.8036 | −0.3497 |
| $^{51}V$ | ±59763 | 62966 | ∓30020 | ∓0.1058 | ±0.4494 | ±0.8871 |
| | −49241 | ∓30020 | 57557 | 0.8700 | −0.3902 | 0.3015 |
| | | | | 81.3[a] | 85.9[a] | 91.1[a] |
| | 30487 | ∓2873 | 1767 | −0.6586 | 0.4252 | 0.6208 |
| $^{31}P$ | ∓2873 | 32119 | 0 | ∓0.4207 | ±0.4760 | ∓0.7723 |
| | 1767 | 0 | 28579 | 0.6239 | 0.7698 | 0.1346 |

[a] MHz.

**Table II. Direction Cosines of Certain Vectors in the Crystal of *trans*-$Cr(CO)_4(PMe_3)_2$ in the $a^*bc$ Axis System**

| vector | direction cosines |
|---|---|
| Cr–P | (0.4554, 0.7373, 0.4991) |
| Cr–C(1) | (0.7241, 0.0087, −0.6896) |
| Cr–C(2) | (−0.4935, 0.6984, −0.5184) |
| bisector of Cr–C(1), Cr–C(2) | (0.8637, −0.4892, −0.1215) |

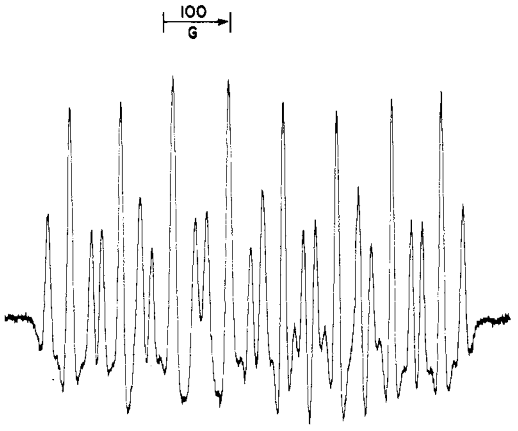

**Figure 1.** Second-derivative EPR spectrum of *trans*-$V(CO)_4(PMe_3)_2$ in a single crystal of *trans*-$V(CO)_4(PMe_3)_2$ at −180 °C for $H_0$ parallel to (0.866, 0, −0.5) in the $a^*bc$ axis system.

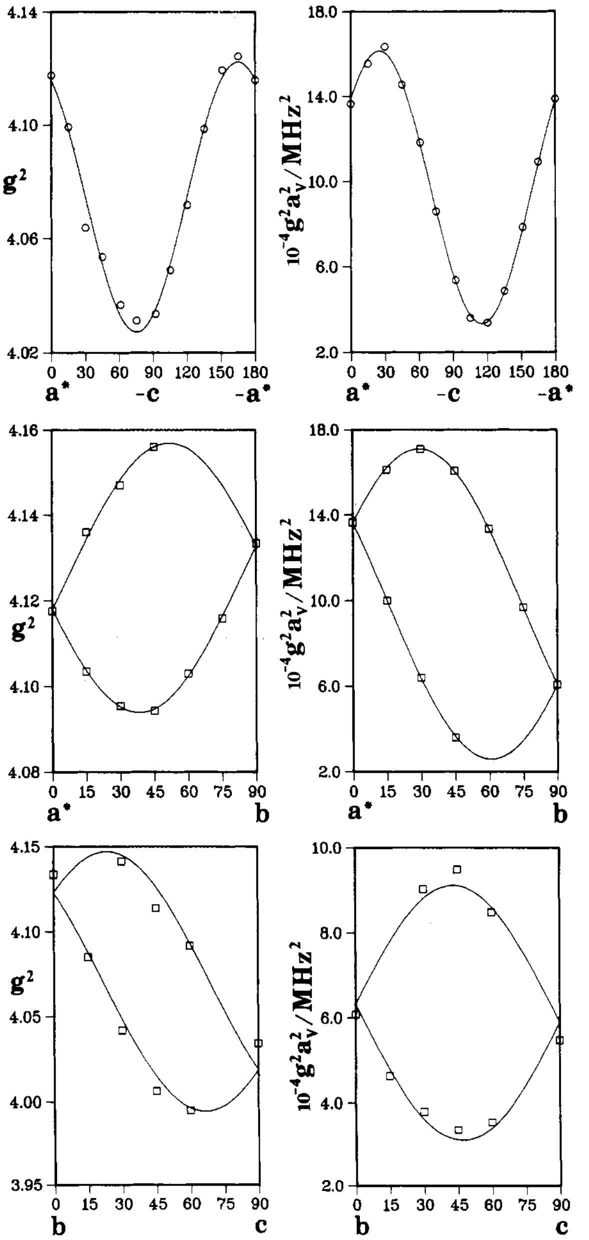

**Figure 2.** Variation of $g^2$ and $g^2a_V{}^2$/MHz$^2$ for the $a^*c$, $a^*b$, and $bc$ planes of a crystal of *trans*-$Cr(CO)_4(PMe_3)_2$ doped with the vanadium analogue.

$R_y$ belongs to the representation $B_{2g}$. The third principal $g$ shift ($\Delta g_{xx}$) will be negative and probably small because the $b_{1g}$ level ($B_{1g} \times B_{2g} \equiv R_x$) is empty and remote. Since the experimentally observed $g$ tensor of *trans*-$V(CO)_4(PMe_3)_2$ is consistent with such a scheme, we conclude that Figure 3d represents the ordering of the energy levels in this molecule.

This model enables us to label the directions of the minimum, intermediate, and maximum principal $g$ factors $x$, $y$, and $z$ respectively. We now seek confirmation of this model in the $^{51}V$ hyperfine interaction and the crystal structure of the host. Referring to Figure 3d, in which we have defined $x$, $y$, and $z$ with the aid of the $g$ tensor only, we note that the semioccupied orbital is $3d_{xz}$. Therefore, we expect maximum $^{51}V$ hyperfine interaction along $y$. Indeed (Table I), the direction of maximum $^{51}V$ hyperfine interaction (218 MHz) is only 16° from $y$ (the very slight anisotropy in the $xz$ plane means that the other principal directions have no significance). This observation tends to confirm the validity of our model, which is further supported by its correlation with Cr–P and Cr–C vectors in the host crystal (Table II). A comparison of these vectors with those in Table I reveals that $z$ ($g = 2.0419$) is roughly parallel to the Cr–P direction (angle 8°), as

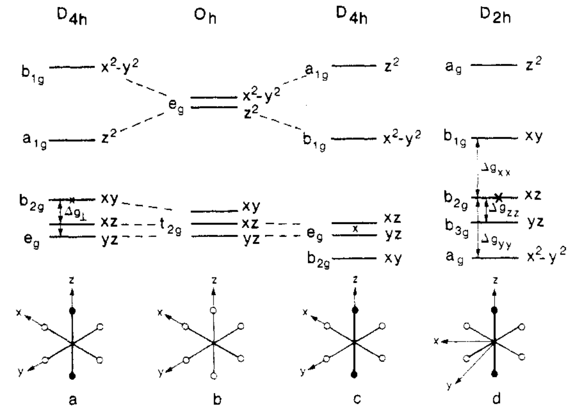

**Figure 3.** The effect on the energy levels of an octahedral molecule of (a) $z$ axis elongation, (c) $z$ axis compression, and (d) distortion to $D_{2h}$ symmetry.

expected. On the other hand, there appears to be no bond direction corresponding to that of the other principal directions of the $g$ tensor. Instead, we note that $g_{\text{int}}$ (2.0244) is only 2.4° from the *bisector* of Cr–C(1) and Cr–C(2), a result which is consistent with the $D_{2h}$ structure of Figure 3d.

Thus, it appears that the *trans*-$V(CO)_4(PMe_3)_2$ impurity occupies a lattice point in the host crystal, and the distortion from $D_{4h}$ conforms to the local symmetry, which is $D_{2h}$. The unpaired electron occupies a $3d_{xz}$ orbital, where $z$ is the PVP direction.

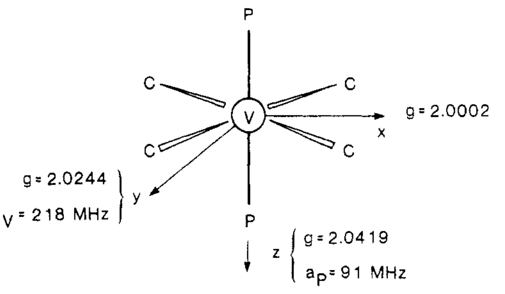

There does not appear to be significant spin population on the $PMe_3$ ligands. The isotropic $^{31}P$ hyperfine interaction, 86 MHz, is only 0.6% of the one-electron parameter $(8\pi/3)g\beta\gamma_n\Psi^2(0)$ for P 3s,[7] and the very small anisotropy indicates a total P 3p spin population of no more than 2%.

The large $^{51}V$ hyperfine interaction along $y$ is due to the coincidence of a negative isotropic (core polarization) term[8] with a negative anisotropic term, $-(4/7)P$. Conversely, along $x$ and $z$ the negative isotropic term is reduced by the positive anisotropic term, (2/7)P, resulting in a small (but probably still negative) hyperfine interaction.

The effective value of $P$, namely, $(7/6)(a_{yy} - {}^1/_2(a_{xx} + a_{zz}))$, is 152 MHz. This figure, being only 35% of $\gamma_e\gamma_n\langle r^{-3}\rangle_{3d}$ obtained from a Hartree–Fock–Slater wave function,[7] implies either surprisingly low V $3d_{xz}$ spin population or a considerable overestimate of the calculated parameter.

**Table III. Comparison of the Spectral Parameters of $V(CO)_6$ and *trans*-$V(CO)_4(PMe_3)_2$**

| | $V(CO)_6{}^a$ | *trans*-$V(CO)_4(PMe_3)_2$ |
|---|---|---|
| $g$ | 1.9789 | $x$ 2.0002 |
| | 2.1121 | $y$ 2.0244 |
| | 2.1370 | $z$ 2.0419 |
| $a_V$/MHz | 69.0 | 83.9 |
| | 157.0 | 218.2 |
| | 128.3 | 91.7 |

[a] References 1–3.

We have seen how the $g$ tensor of *trans*-$V(CO)_4(PMe_3)_2$ can be accommodated by a tetragonal compression along $z$ (the PVP direction) followed by a "scissors" distortion of the CVC angles to $D_{2h}$ symmetry. What about $V(CO)_6$ itself? We know that in the pure compound there is a tetragonal compression,[9] the axial V–C bonds being shorter than the equatorial by 0.012 Å. Bratt et al.[3] consider the dominant distortion to be the "scissors" distortion to $D_{2h}$ and place the $a_g$ $(x^2 - y^2)$ orbital above the $b_{2g}$ $(xz)$ and $b_{3g}$ $(yz)$ orbitals in Figure 3d. The ground state of $V(CO)_6$, under this hypothesis, is $^2A_g$ in $D_{2h}$ symmetry. The unpaired electron is essentially in $d_{x^2-y^2}$, and $z$ becomes the direction of minimum $g$ (1.9789). With a negative isotropic $^{51}V$ hyperfine interaction via spin polarization and a negative $-(4/7)P$ anisotropic contribution, we would expect minimum $g$ (1.9789) to be associated with maximum (negative) $^{51}V$ hyperfine interaction and (Table III) it is not. Of course, spin population in V 4s was invoked[3] to provide a positive isotropic $^{51}V$ hyperfine contribution. At this stage we merely wish to point to our interpretation of the spectrum of *trans*-$V(CO)_4(PMe_3)_2$ and suggest that it may also apply to $V(CO)_6$.

The main difference between the two cases lies in the anisotropic components of the $^{51}V$ hyperfine tensors. Subtracting out the (negative) isotropic contributions, these are (Table III) for $V(CO)_6$ 49, −39, and −10 MHz and for *trans*-$V(CO)_4(PMe_3)_2$ 47, −87, and 39 MHz along the $x$, $y$, and $z$ axes, respectively. As we have seen, the latter is an almost axial tensor identifiable with the $d_{xz}$ orbital. In fact the $^{51}V$ hyperfine anisotropy in *trans*-$V(CO)_4(PMe_3)_2$ can be broken down into two precisely axial contributions: 45, −90, 45 $(d_{xz})$ and 4, 4, −8 $(d_{xy})$. In the case of $V(CO)_6$ the $d_{xy}$ contribution (20, 20, −40 MHz) has increased at the expense of that from $d_{xz}$ (30, −60, 30 MHz). Thus it could be argued that in *trans*-$V(CO)_4(PMe_3)_2$ the energy levels are further apart than in $V(CO)_6$. As a result, admixture (via the spin–orbit interaction) of the $B_{1g}$ state $(d_{xy})$ into the ground $B_{2g}$ $(d_{xz})$ state is much less in *trans*-$V(CO)_4(PMe_3)_2$ than in $V(CO)_6$.

In summation, our results for *trans*-$V(CO)_4(PMe_3)_2$ in a single crystal of the chromium analogue suggest a $B_{2g}$ $(d_{xz})$ ground state. We have also shown that a $B_{2g}$ $(d_{xz})$ ground state (albeit badly adulterated by the $B_{1g}$ state) can accommodate the data for $V(CO)_6$.

**Registry No.** *trans*-$V(CO)_4(PMe_3)_2$, 17548-29-7; *trans*-$Cr(CO)_4(PMe_3)_2$, 30513-08-7.

---

[7] Morton, J. R.; Preston, K. F. *J. Magn. Reson.* **1978**, *30*, 577.

[8] Symons, M. C. R. "Chemical and Biochemical Aspects of Electron-Spin Resonance Spectroscopy"; Wiley: New York, 1978; Chapter 12.

[9] Bellard, S.; Rubinson, K. A.; Sheldrick, G. M. *Acta Crystallogr., Sect. B: Struct. Crystallogr. Cryst. Chem.* **1979**, *B35*, 271.